3-aminopropyltriethoxysilanes Modified Porous Silicon as a Voltammetric Sensor for Determination of Silver Ion

ShaoYuan Li[1,2], WenHui Ma[1,2], Yang Zhou[1,2*], XiuHua Chen[3], MingYu Ma[1,2],YaoHui Xu[1,2], Zhao Ding[1,2], XingHui Wu[3]*

[1] National Engineering Laboratory for Vacuum Metallurgy, Kunming University of Science and Technology, Kunming 650093, China
[2] Faculty of Metallurgical and energy engineering, Kunming University of Science and Technology, Kunming 650093, China
[3] Faculty of Physical Science and Technology, Yunnan University, Kunming 650091, China
*E-mail: mwhsilicon@163.com; zhouyangnano@163.com

A novel voltammetric sensor based on 3-aminopropyltriethoxysilanes (APTES) modified porous silicon electrode (APTES-PSE) was elaborated and used for determinating Ag^+ in aqueous solution. Fourier transform infrared (FTIR) spectroscopy was performed to confirm the modification of APTES. The surface morphologies of PSE and APTES-PSE were characterized by atom force microscopy (AFM). Electrochemical property of PSE and modified electrode was studied using electrochemical impedance spectroscopy (EIS). Under the optimal experimental conditions, the cathode peak current intensity of APTES-PSE linearly changes with logarithm of Ag^+ concentrations over the wide range from 1×10^{-3} mol L^{-1} to 1×10^{-7} mol L^{-1}, with a detection limit of 3×10^{-8} mol L^{-1}. Meanwhile, the APTES-PSE showed a good sensitive to Ag^+ in the aqueous solution and which is attributed to the preferential chelation of N atoms of APTES. These results suggest that the choice of PSE as the substrate of the voltammetric sensor might be a very promising means for integrated analytical sensing.

Keywords: Porous silicon electrode, Surface modification, Voltammetric sensor, Silver ion detection

1. INTRODUCTION

Porous silicon (PS) is a promising material which has attracted considerable widespread attentions, because its specific surface is large and it is compatible with integrated silicon-based IC technology. These unique features aroused the interests of the design of silicon based sensors which used PS base hybrid material as sensing layer. PS has been utilized in gas sensor [1-4], biomolecular

sensor [5], organic molecule sensor [6-7] and ion sensor [8], etc. However, PS has not widely been used to detect metal ions especially for Ag^+.

Silver ions were extensively utilized in the photographic and imaging industry. The effluent containing Ag^+ was discharged to the environment which leaded to the possibility for exposure to aquatic and terrestrial organisms. Recently, its potential toxicity has drawn people's attentions and determination of Ag^+ in industrial and environmental samples is becoming more important. Several analytical techniques were applied to determinate Ag^+ in food, water and real samples, including atomic emission spectroscopy (AES) [9,10], atomic absorption spectrometry (AAS) [11,12],inductively coupled plasma mass spectrometry (ICP-MS) [13,14], spectrophotometry [15], etc. However, these techniques are commonly utilized in the laboratory and require professional skills.

Voltammetric sensors are the most favorable tool for metal ions determination because of their remarkable sensitivity, simple equipment and low cost. The chemically modified electrodes (CMEs) can improve both sensitivity and selectivity of voltammetric sensor. Thus they are considered to be more suitable for application in voltammetric sensors. The CMEs have received increasing attentions in recently years and been applied to determinate trace metal ions. Usually the carbon paste electrode [16,17], glassy carbon electrode [18,19] and precious metal electrode [20,21] were usually choosed as the substrate of the voltammetric sensor. In this paper, A novel voltammetric sensor was fabricated by porous silicon (PS) modified with 3-aminopropyltriethoxysilanes (APTES) and successfully used for the determination of Ag^+ in the aqueous solution. Cyclic voltammogram was performed to study the electrochemical behaviors of the Ag^+ chelated by APTES-PSE. Meanwhile, the electrochemical property of PSE and modified electrode was carefully studied by electrochemical impedance spectroscopy (EIS).

2. EXPERIMENTAL PART

2.1 Reagents and Apparatus

Single crystal silicon wafers were purchased from 46th Institute of Semiconductor of China. All chemicals used were of analytical reagent grade. Aqueous solutions were prepared with deionised water (18.25 $\Omega \cdot cm$). Hydrofluoric acid (40 wt.%), ethanol and toluene were all purchased from China National Medicines Corporation Ltd. Acetic acid, sodium acetate, potassium dihydrogen phosphate, potassium nitrate, ammonium chloride, ammonia and all of the metal salt was from TianJing chemical reagent Factory. 3-aminopropyltriethoxysilanes (APTES) was purchased from Sigma Aldrich.

All reagents were analytical grade and were used without further purification. A Stock solution of 1 mM $AgNO_3$ was prepared and stored in the dark. Different concentration of standard solution of Ag^+ was obtained by dilution of the stock solution.

The electrochemical measurements were performed by CHI660C electrochemical analytical instrument (CH Instrument Co, Shanghai, China). The immobilization of APTES was confirmed by FTIR spectrum that was collected by Bruker model EQUINOX 55 Fourier Transform Infrared

instrument (Germany). The surface morphology of the PSE and APTES-PSE was studied by the 5500 model atomic force microscope (Agilent, United States)

2.2 Preparation of Modified PS Electrode

Silicon samples $1\times1cm^2$ were cut from double side polished, (100)-oriented, p-type silicon wafers (resistivity 0.01-0.09 $\Omega\cdot$cm). They were cleaned in ethanol and distilled water for 10 min under sonication, respectively. The native oxide was removed by immersing the samples in 10 wt.% HF aqueous for 5 min. The treated wafers were installed in the self-made Teflon apparatus (as shown in scheme 1), and two platinum plates were used as the counter electrode. PS electrode was prepared by anodizing the wafer in 1:5:1 (v:v:v) mixed solutions of 40 wt.% HF, absolute ethanol and deionised water at a current density of 30 mA cm^{-2} for 20 min. After etching, the electrode was rinsed with absolute ethanol and then photochemically oxidized under a low pressure mercury arc lamp [22].

The oxidized PS reacted with 10% (v:v) APTES in toluene for 12 h. The reaction was refluxed at 80 ^{0}C under N_2 with stirring agitation. The resultant APTES-PSE was washed by ethanol and deionized water twice and then dried under a stream of dry N_2.
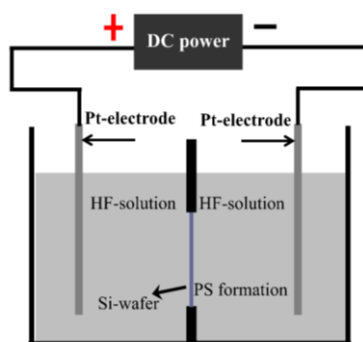
Scheme 1. Schematic of the electrochemical cell with two Pt electrodes

2.3 Analysis procedure

Preconcentration was carried out by dipping the modified electrode into AgNO3 solution which contained a certain number of Ag^+. The solution was stirred under the dark. After the preconcentration, the APTES-PSE was washed thoroughly by deionized water and then cyclic voltammogram measurements were conducted immediately. A traditional three-electrode system was used in the measurements, comprising a modified working electrode, a platinum auxiliary electrode, and a saturated calomel electrode (SCE). The supporting electrolyte was a silver-free solution and was degassed with N_2 for approximately 5 min prior to data acquisition. All experiments were carried out at room temperature (25 ± 1 °C). The preparation and measurement process of APTES-PSE is indicated in Scheme 2.
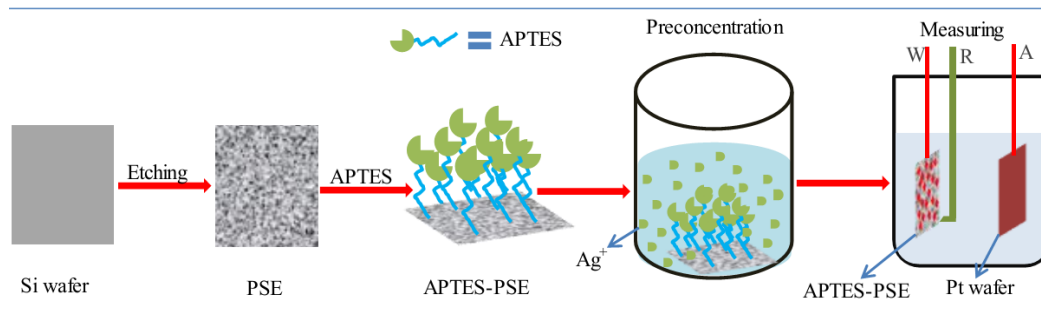
Scheme 2. Schematic illustration of the preparation and measurement process of APTES-PSE.

3. RESULTS AND DISCUSSION

3.1 FTIR spectrum of APTES-PSE

The freshly prepared PSE covered by silicon hydrogen species (SiH_x, x = 1, 2, 3) was demonstrated by previous investigators [23,24]. In the Fig. 1A, the absorption band at about 2100 cm^{-1} verifies the existence of SiH_x groups. Hydroxyl groups (Si-OH) are indispensable species for the immobilization of APTES on the PSE surface. After the modification of APTES, some dramatic changes are observed in the FTIR spectrum of the APTES-PSE (Fig. 1B). The double peaks at 3361.89 cm^{-1} and 3296.31 cm^{-1} are due to $-NH_2$ stretching mode. And the board absorption band between 1600 and 1660 cm^{-1} is designated as the deformation mode of $-NH_2$. The strong bands at 2935.82 cm^{-1} and 2871.91 cm^{-1} are assigned to stretching mode of $-CH_2$ [25]. The absorption band at 1160 cm^{-1} is caused by stretching mode of Si-O-Si [26]. These results suggest that APTES is successfully anchored on the PSE surface.
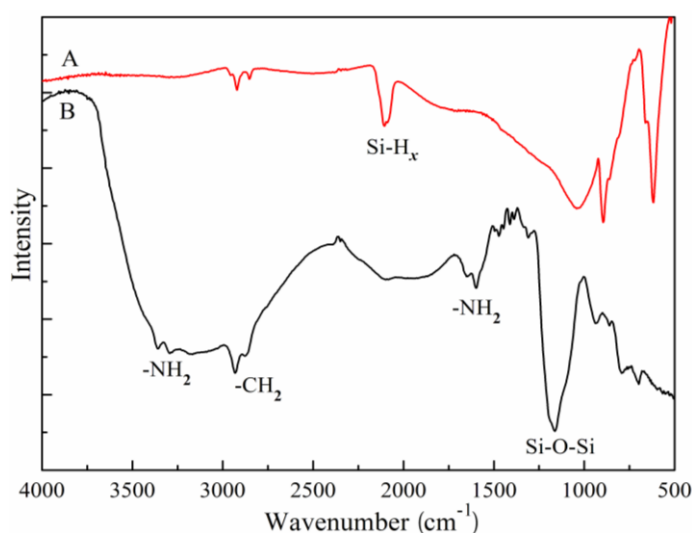

Figure 1. FTIR spectrum of PSE (A) and APTES-PSE (B).

3.2 Structural characterization of PSE and APTES-PSE

AFM imaging provided detail information about the surface morphology of modified electrode. The AC mode AFM images of PSE and APTES-PSE were shown in Fig. 2.

We can found that the PSE surface is covered by a honeycomb-like porous layer, about 100 ± 20 nm in diameter (Fig. 2A). Fig. 2B shows the morphology of APTES-PSE. After the modification, the honeycomb-like pores are not obviously observed. The height distribution of hillocks on the samples is counted, the distribution ranges from 100 to 120 nm for PSE. The APTES-PSE has a wider range, from 180 to 280 nm. Meanwhile, the roughness of samples has a sharp increase from 12.2 to 42.2 nm.
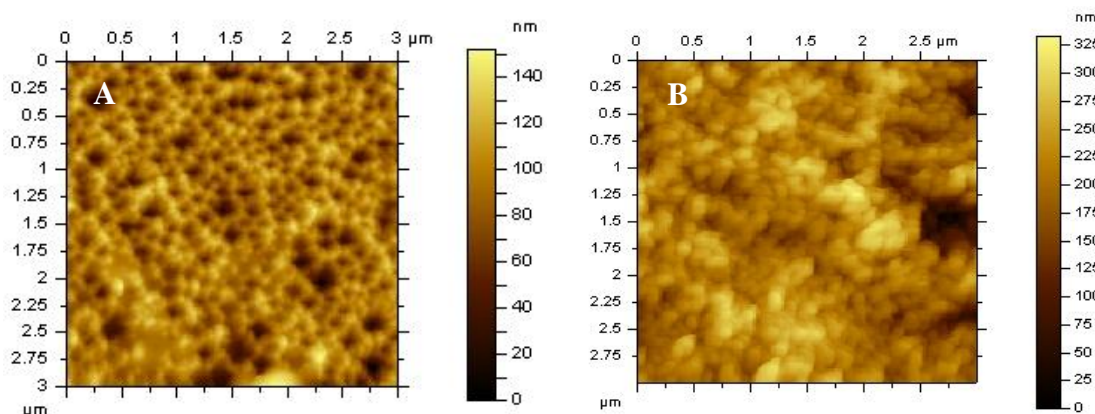

Figure 2. AFM micrographs of PSE (A) and APTES-PSE (B).

3.3 Electrochemical impedance spectroscopy of PSE and APTES-PSE

Electrochemical impedance spectroscopy (EIS) is an efficient tool to characterize the interfacial properties of the electrochemical electrodes. As known, the charge transfer resistance (R_{ct}) controls the electron transfer rate of the redox probe at the solution/electrode interface. It varies when different species are immobilized on the electrode surface [27]. The value can be expediently obtained from the semicircle diameter at higher frequency range in Nyquist plot of EIS.
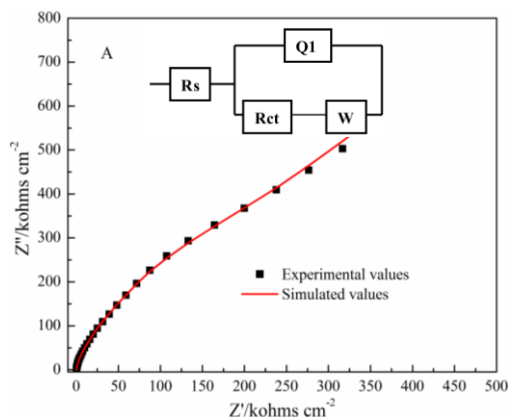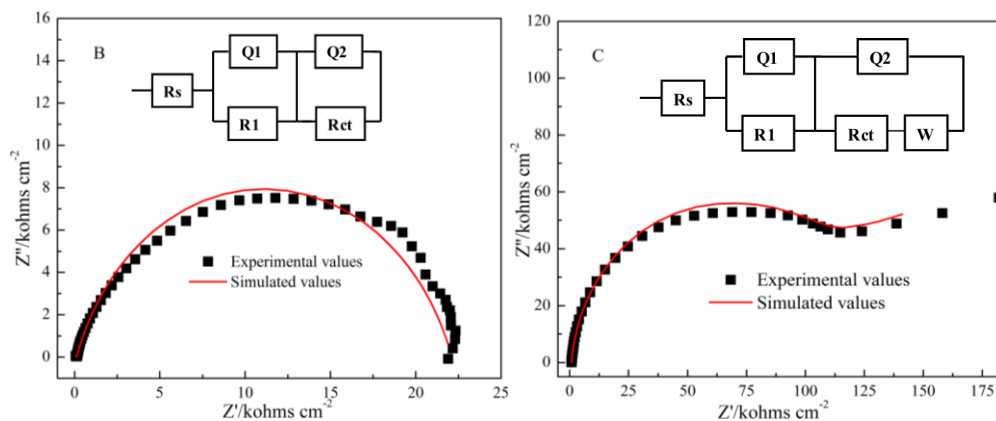
Figure 3. Niquist and equivalent circuit (insert) of Si electrode, PSE (A) and APTES-PSE (B) in aqueous 0.2 mol L^{-1} KNO_3 solution containing 1 mmol L^{-1} $Fe(CN)_6^{3-/4-}$. Perturbation amplitude: 5 mV.

In our case, the impedance measurements of Si electrode, PSE and APTES-PSE were performed in the frequency domain 10 mHz-100 kHz. The Niquist plots of the sample are shown in Fig. 3, which are recorded in 0.2 mol L^{-1} KNO_3 solution containing 1 mmol L^{-1} $Fe(CN)_6^{3-/4-}$. Nyquist diagram for Si electrode shown in the Fig. 6 includes a part of the big semicircle at Z_{re} axis high-frequency region, followed by a Warburg line. The linear part at low-frequency region represented the diffusion control process [27], the semicircle part observed at high frequency corresponds to the charge transfer process and is known as charge transfer resistance (R_{ct}). A higher radius of the semicircle means a larger charge transfer resistance [28], it will lead to a difficult electrochemical process, which is attributed to the high resistance nature of silicon. Compared with the Si electrode, the PSE contains a smaller R_{ct} (21.99 kΩ) which is also in line with previous impedance data in that electrical impedance of PS is much lower than that of bare Si [29]. Meanwhile, we can find that the redox process occurs on the porous electrode is only controlled by the charge transport process. In our case, the impedance behavior of the PS electrode doesn't in line with the model of porous electrode proposed by de Levie [30]. Thus, the Niquist plot of PSE can't fitted by the by the transmission line model (TLM) [31], it may be attributed to the poor electroconductivity of PS and which don't satisfy the assumption of metallic electrode behavior with infinite conductivity [32]. From the Fig. 3C, we can find that the modification of APTES leads to an increase of R_{ct} (131.5 kΩ) and the presence of Warburg line at the low frequency region, these shows that the APTES film acts as a block layer for electron and mass transfer. This behavior also indicated that the APTES was successfully immobilized on the PSE surface.

To clarify the relationship between the impedance response of PSE and APTES-PSE surface structure, the impedance data are analyzed using the equivalent circuit consisting of minimum number of elements which fit the whole set of impedance data with fair precision (the discrepancy between experiment data and theoretical data is less than 2%). As the simulation results, we obtain the corresponding equivalent circuits for the research electrode. The equivalent circuit of silicon wafer electrode consists of a pair Rct-Q1, representing the elements of the double layer at the silicon/electrolyte surface, where Q1 is a constant phase element. However, for the PS electrode, the

additional R1-Q1 is caused by the porous structure. A Warburg resistance W is introduced when the APTES is grafted onto the PS surface.

3.4 Optimization of APTES-PSE

In order to obtain the largest peak current and well defined peak shape of the redox, the preconcentration and measurement conditions were simultaneously studied during optimization. The pH of preconcentration solution affected the solubility of metal ions and the ionization state of functional groups. The effect of pH and accumulation time on cathode peak current intensity was investigated, and the results were shown in Fig.4.
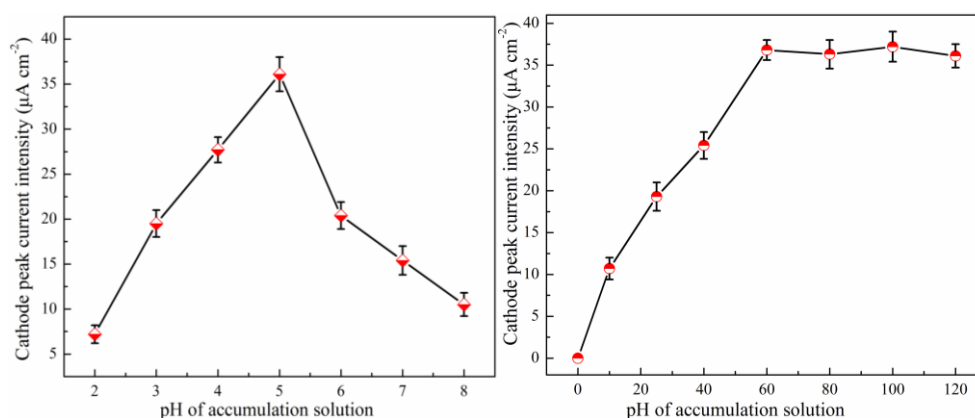
Figure 4. The effect of pH of accumulation solution and accumulation time on the cathode peak current intensity. Measurement conditions: support electrolyte: 0.1 mol L^{-1} KNO_3, scan rate: 100 mV s^{-1}.

In our experiment, the pH was adjusted using 0.1 M HNO_3 and 0.1 M NaOH. At first the cathode peak current height had an increase with the increasing pH, which increases to 36 $\mu A/cm^2$ at the pH 5. But, a decreasing current intensity follows as the continued growth in pH. From the plot of t-Ipc (right), we can find that the cathode peak current has a faster increase in the first 20 minutes, and which increases to stable value (about 36.7 $\mu A/cm^2$) when the accumulation time is 60 min. Thus, the pH 5 and the accumulation time 60 min is choosed as optimal silver ions preconcentration condition in the follow-up experiment.

After the preconcentration, the APTES-PSE was washed thoroughly by deionized water and then cyclic voltammogram measurements were conducted immediately. Five different supporting electrolytes (NH_4Cl/NH_3 buffer, HNO_3, HAC/NaAC, NaH_2PO_4 and KNO_3) were tested to obtain the best peaks. The optimal supporting electrolyte was found to be 0.1 mol L^{-1} KNO_3. The support electrolyte was degassed with N_2 for approximately 5 min prior to data acquisition.

3.5 Cyclic voltammogram behavior of Ag+ on the APTES-PSE

The cyclic voltammogram was performed to study the electrochemical behavior of Ag^+ on the APTES-PSE. As shown in Fig. 5, no peak can be discerned over the whole form -600 mV to 800 mV when the APTES-PSE is tested before the preconcentration (red dot line in Fig. 5). However, A pair of redox peaks are respectively observed at E_{pa} = 180 mV and E_{pc} = -142 mV when a certain number of Ag^+ is enriched on the APTES-PSE. The reduction of chelated Ag^+ in negative potential indicates that the reduction process is a relatively difficult step, which is attributed to the difficult electron and mass transfer on the solution/electrode interface. This difficulty is caused by the high impedance and interlaced nano-level channels of modified PSE. Li at el. [33] observed the similar reduction potential in Ag^+-zeolite modified electrode. The peak potential separation, ΔE_p ($\Delta E_p = E_{pa} - E_{pc}$, 322 mV) far outweighs 59 mV expected for a reversible system [34]. Thus, we infer that the redox of Ag^+ chelated by APTES is inferred as a quasi-reversible process.
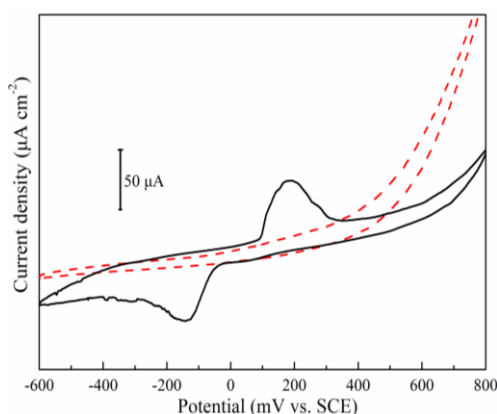

Figure 5. Cyclic voltammogram of APTES-PSE in 0.1 molL-1 KNO_3 before (red dot line) and after (black line) Ag^+ preconcentration in 1×10^{-4} molL^{-1} solution at pH = 5, scan rate: 100 mV s^{-1}.

3.6 The relationship between peak current and Ag+

To investigate the dynamic response range of APTES-PSE, a series of different concentrations of $AgNO_3$ were used as preconcentration solutions under the optimized working conditions described above. Fig. 6A shows that the cathode peak current intensity ($|I_{pc}|$) increases with concentration of Ag^+. The calibration plot in Fig. 6B highlights a linear response for logarithmic Ag^+ concentrations over the range from 1×10^{-3} mol L^{-1} to 1×10^{-7} mol L^{-1}.

The linear equation is:

$$|I_{pc}| \ (\mu A \ cm^{-2}) = 118.28 + 15.15 \times lgCAg^+ \quad (C_{Ag+}/mol \ L^{-1}) \quad (R^2 = 0.97173)$$

A similar linearity between i and $lgCAg^+$ over the range 1×10^{-8} to 1×10^{-4} mol L^{-1} also was observed on polypyrrole film modified glassy carbon electrodes [35]. The logarithmic nature of the calibration plot can be related to saturation of the modification film with silver species. This effect is

particularly pertinent for adsorptive type processes [36,37]. The sensitivity, expressed as the slope of the linear region of the calibration curve [38], was observed as 15.15 $\mu A/$ lgC ($C_;$ mol L^{-1}). The relative standard deviation (%R.S.D., N = 6) for 1×10^{-4} mol L^{-1} Ag$^+$ was 2.57%, which demonstrated the reproducibility of the APTES-PSE. The limit of detection (LOD) was calculated as the usual method, namely, S/N = 3. The value was determined as 3.0×10^{-8} mol L^{-1}. Even though which is not better than that of many other researcher [35,39,40], the compatibility of PSE with silicon-base IC is very promising for integrated analytical sensing.
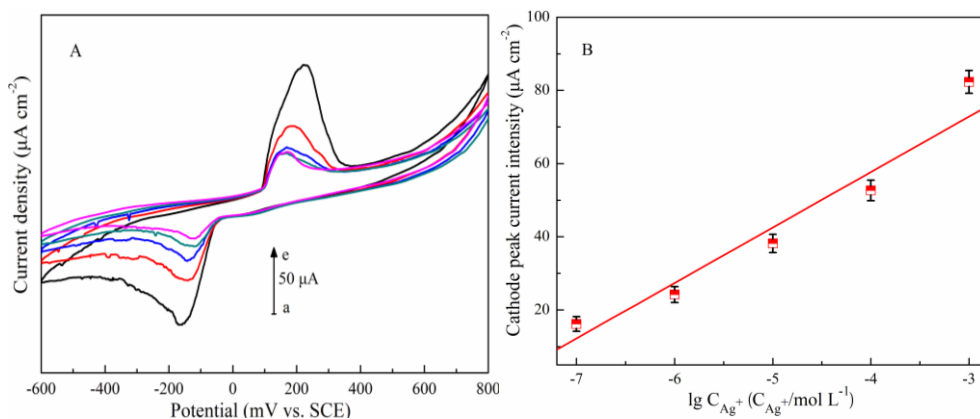

Figure 6. (A) Cyclic voltammograms of APTES-PSE in 0.1molL^{-1} KNO$_3$ after preconcentration of various concentrations: (a) 1×10^{-3}molL^{-1}, (b) 1×10^{-4}molL^{-1}, (c) 1×10^{-5}molL^{-1}, (d) 1×10^{-6}molL^{-1}, (e) 1×10^{-7}molL-1. Conditions: preconcentration time: 60 min, pH = 5, scan rate: 100 mV s^{-1}. (B) Calibration plot of cathode current intensity versus concentrations of Ag$^+$.

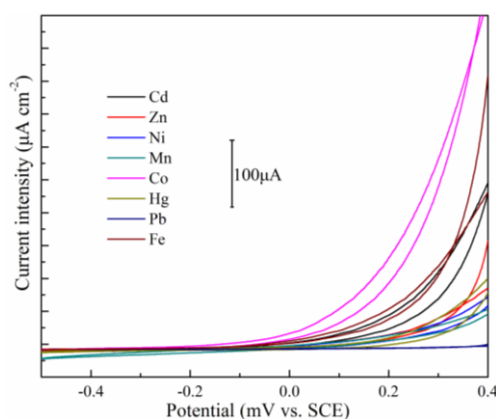*3.7 Effects of interfering metal ions on APTES-PSE*

Figure 7. Cyclic voltammograms of APTES-PSE in 0.1 mol L^{-1} KNO$_3$ after preconcentration of various metal species (Cd^{2+}, Co^{2+}, Pb^{2+}, Ni^{2+}, Zn^{2+}, Hg^{2+}, Fe^{2+} and Mn^{2+}). Conditions: concentration: 1×10^{-4} mol L^{-1}; pH = 5; preconcentration time: 60 min; scan rate: 100 mV s^{-1}.

In order to test the selectivity, the APTES-PSE was used to detect different metal ions. The modified electrode was immersed in solution containing 1×10^{-4} mol L^{-1} of foreign metal ions (Cd^{2+},

Co^{2+}, Pb^{2+}, Ni^{2+}, Zn^{2+}, Hg^{2+}, Fe^{2+} and Mn^{2+}). The preconcentration conditions were just the same as that of Ag^+. After the preconcentration, the electrochemical measurements were carried out and the results were shown in Fig. 7.

It can be observed that the modified electrode wasn't sensitive absolutely to Cd^{2+}, Co^{2+}, Pb^{2+}, Ni^{2+}, Zn^{2+}, Hg^{2+}, Fe^{2+} and Mn^{2+} ions. The cyclic voltammograms behavior of APTES-PSE-M (M represents various metal species) is similar to that (red dot line) of the APTES-PSE in Fig. 5. Thus, we can deduce that the foreign metal ions don't chelate with APTES. Furthermore, the coexisting interference of the above-mentioned metal ions was studied by analyzing sample solution containing a fixed amount of Ag^+ (1×10^{-5} mol L^{-1}) and excess foreign species. The results showed that 50-fold foreign species scarcely influenced the cathode peak current intensity of Ag^+, which may be attributed to the N atom of NH_2 in APTES, the similar selectivity to Ag^+ given by NH_2 has been reported by previous researcher [40,41].

4. CONCLUSIONS

A novel electrochemical voltammetric sensor based on APTES modified PS was proposed to determine Ag^+ by using cyclic voltammetry. The AFM characterization showed the porous structure was covered by the APTES graft. The electrochemical impedance data of the PSE and APTES-PSE showed that the porous layer can lead to form additional R1-Q1 element and the APTES film acts as a block layer for electron and mass transfer during the redox of probe. The detection conditions of the APTES-PSE were optimized and the results showed that preconcentration time 60 min and pH of solution 5.0 can obtain the optimal detection result. Under the optimal experimental conditions, the cathode peak current intensity of APTES-PSE linearly changed with logarithmic Ag^+ concentrations over the wide range from 1×10^{-3} mol L^{-1} to 1×10^{-7} mol L^{-1} and with a detection limit of 3×10^{-8} mol L^{-1}. Meanwhile, the APTES-PSE showed a good sensitive to Ag^+ in the aqueous solution, which was attributed to the preferential chelation given by N atom of NH_2.

References

1. J. Kanungo, H. Saha and S. Basu, *Sens. Actuators: B*, 140 (2009) 65.
2. M. Rocchia, E. Garrone and F. Geobaldo, *Phys. Status Solidi (a)*, 197 (2003) 365.
3. S. E. Lewis, J. DeBoer, J. L. Gole and P. J. Hesketh, *Sens. Actuators: B*, 110 (2005) 54.
4. S. Ozdemir, T. B. Osburn and J. L. Gole, *J. Electrochem. Soc.*, 158 (2011) J201.
5. S. D. Alvarez, A. M. Derfus, M. P. Schwartz, S. N. Bhatia and M. J. Sailor, *Biomaterials*, 30 (2009) 26.
6. G. G. Salgado, T. D. Becerril and H. J. Santiesteban, E. R. Andrés, *Opt. Mater.*, 29 (2006) 51.

7.   M. Archer, M. Christophersen and P. M. Fauchet, *Sens. Actuators: B*, 106 (2005) 347.
8.   S. Zairi, C. Martelet, N. Jaffrezic-Renault, R. Lamartine, R. M'gaïeth, H. Maarefc, M. Gamoudid and G. Guillaudd, *Appl. Surf. Sci.*, 172 (2001) 225.
9.   K. S. Choi, C. H. Lee, J. G. Kim, W. H. Kim and J. G. Kang, *Talanta*, 71 (2007) 662.
10. N. P. Zaksas, T. T. Sultangazieva and V. A. Gerasimov, *Anal. Bioanal. Chem.* 391 (2008) 687.
11. E. Macalalad, R. Bayoran, B. Ebarvia and I. Rubeška, *J. Geochem. Explor.*, 30 (1988) 167.
12. G. Chakrapani, P. L Mahanta, D. S. R Murty and B. Gomathy, *Talanta*, 53 (2001) 1139.
13. K. Ndung'u, M. A. Ranville, R. P. Franks and A. R. Flegal, *Mar. Chem.*, 98 (2006) 109.
14. B. Wu, I. Susnea, Y. Chen, M. Przybylski and J. S. Becker, International, *J. Mass Spectrom.*, 307 (2011) 85.
15. A. Rouis, R. Mlika, C. Dridi, J. Davenas, H. B. Ouada, H. Halouani, I. Bonnamour and N. Jaffrezic, *Mat. Sci. Eng. C*, 26 (2006) 247.
16. B. Pekec, A. Oberreiter, S. Hauser, K. Kalcher, A. Ortner, *Int. J. Electrochem. Sci.*, 7 (2012) 4089.
17. E. M. Ghoneim, Talanta, 82 (2010) 646.
18. B. Ntsendwana, B.B. Mamba, S. Sampath, O.A. Arotiba , Int. J. Electrochem. Sci., 7 (2012) 3501.
19. H. Zhao, Y. Jiang, Y. R. Ma, Z. J. Wu, Q. Cao, Y. J. He, X. G. Li and Z. B. Yuan, Electrochim. Acta, 55 (2010) 2518.
20. A. Giacomino, O. Abollinoa, M. Lazzaraa, M. Malandrino and E. Mentasti, Talanta, 83 (2011) 1428.
21. Y. Bonfil, M. Brand and E. Kirowa-Eisner, *Anal. Chim. Acta*, 464 (2002) 99.
22. S. Belhousse, R. Boukherroub, S. Szunerits, S. Gabouze, A. Keffous, S. Sam and A. Benaboura, *Surf. Interface Anal.*, 42 (2010) 1041.
23. P. Gupta, V. L. Colvin and S. M. George, *Phys. Rev. B*, 37 (1988) 8234.
24. G. Mattei, V. Valentini and R. Polini, *Phys. Status. Solidi. (c)*, 4 (2007) 2049.
25. R. S. Bai and T. E. Abraham, *Water Res*., 36 (2002) 1224.
26. Be. Mahmoudi, N. Gabouze, L. Guerbous, M. Haddadi and K. Beldjilali, *J. Lumin.*, 127 (2007) 534.
27. R. K. Sharma, A. C. Rastogi and S. B. Desu, *Physica B*, 388 (2007) 344.
28. J. R. Macdonald, *J. Electroanal. Chem.*, 223 (1987) 25.
29. D. Vanmaekelbergh and P. C. Searson, *J. Electrochem. Soc.*, 141 (1994) 697.
30. R. de Levie, Adv. Electrochem. *Electrochem. Eng.*, 6 (1967) 329.
31. M. Itagaki, Y. Hatada, I. Shitanda and K. Watanabe, *Electrochim. Acta*, 55 (2010) 6255.
32. O. E. Barcia, E. D'Elia, I. Frateur, O. R. Mattos, N. Pe´be`re and B. Tribollet, *Electrochim. Acta*, 47 (2002) 2109.
33. Y. J. Li and C. Y. Liu, *Imaging Sci. Photochem.*, 20 (2002) 111.
34. A. J. Bard and L. R. Faulkner, *Electrochemical Methods: Fundamentals and Applications*, Wiley, New York, (2000)
35. A. R. Zanganeh and M. K. Amini, *Electrochimica Acta*, 52 (2007) 3822.
36. N. L. Pickup, J. S. Shapiro and D. K. Y. Wong, *Anal. Chim. Acta*, 364 (1998) 41.
37. F. Y. Song and K. K. Shiu, *J. Electroanal. Chem.*, 498 (2001) 161.
38. N. Daud, N. A. Yusof, T. W. Tee and A. H. Abdullah, Int. *J. Electrochem. Sci.*, 7 (2012) 175.
39. G. P. Yan, Y. H. Wang, X. X. He, K. M. Wang, J. Su, Z. F. Chen and Z. H. Qing, *Talanta*, 94 (2012) 178.
40. Q. Y. Liu, F. Wang, Y. H. Qiao, S. H. Zhang and B. X. Ye, *Electrochim. Acta*, 55 (2010) 1795.
41. L. M. Huang, W. H. Liao, H. C. Ling and T. C. Wen, *Mater. Chem. Phys.*, 116 (2009) 474.